Magnetic structure and critical behavior of GdRhIn$_5$: Resonant x-ray diffraction and renormalization group analysis

E. Granado,[1,2,*] B. Uchoa,[2] A. Malachias,[2] R. Lora-Serrano,[1] P. G. Pagliuso,[1] and H. Westfahl, Jr.[2]

[1]*Instituto de Física "Gleb Wataghin," UNICAMP, Caixa Postal 6165, 13083-970 Campinas, SP, Brazil*

[2]*Laboratório Nacional de Luz Síncrotron, Caixa Postal 6192, 13084-971 Campinas, SP, Brazil*

The magnetic structure and fluctuations of tetragonal GdRhIn$_5$ were studied by resonant x-ray diffraction at the Gd L_{II} and L_{III} edges, followed by a renormalization group analysis for this and other related Gd-based compounds, namely Gd$_2$IrIn$_8$ and GdIn$_3$. These compounds are spin-only analogs of the isostructural Ce-based heavy-fermion superconductors. The ground state of GdRhIn$_5$ shows a commensurate antiferromagnetic spin structure with propagation vector $\vec{\tau} = (0, \frac{1}{2}, \frac{1}{2})$, corresponding to a parallel spin propagation along the $\vec{a}$ direction and antiparallel propagation along $\vec{b}$ and $\vec{c}$. The spin direction lies along $\vec{a}$. A comparison between this magnetic structure and those of other members of the $R_m(\mathrm{Co,Rh,Ir})_n\mathrm{In}_{3m+2n}$ family (R=rare earth, $n=0,1$; $m=1,2$) indicates that, in general, $\vec{\tau}$ is determined by a competition between first- (J_1) and second-neighbor (J_2) antiferromagnetic (AFM) interactions. While a large J_1/J_2 ratio favors an antiparallel alignment along the three directions (the G-AFM structure), a smaller ratio favors the magnetic structure of GdRhIn$_5$ (C-AFM). In particular, it is inferred that the heavy-fermion superconductor CeRhIn$_5$ is in the frontier between these two ground states, which may explain its noncollinear spiral magnetic structure. The critical behavior of GdRhIn$_5$ close to the paramagnetic transition at $T_N=39$ K was also studied in detail. A typical second-order transition with the ordered magnetization critical parameter $\beta=0.35$ was experimentally found, and theoretically investigated by means of a renormalization group analysis. Although the Gd $4f^7$ electrons define a half-filled, spherically symmetrical shell, leading to a nearly isotropic spin system, it is argued that a significant spin anisotropy must be claimed to understand the second order of the paramagnetic transition of GdRhIn$_5$ and the related compound Gd$_2$IrIn$_8$.

PACS number(s): 75.25.+z, 75.40.Cx, 75.50.Ee, 61.10.Nz

I. INTRODUCTION

The recent discovery of a new class of heavy-fermion superconductors, Ce$_m$(Co,Rh,Ir)$_n$In$_{3m+2n}$ ($n=0,1$; $m=1,2$),[1–5] has triggered extensive research on their physical properties. While it is well established that the spin fluctuations are key ingredients to determine the superconductivity in this family,[6] the details of the pairing mechanism are not presently known.[7] Nonetheless, the relatively large critical temperatures found for some compounds ($T_c=2.3$ K for tetragonal CeCoIn$_5$ is a record-high value for Ce-based heavy fermion systems), and the evolution of this property with the ratio of c and a lattice parameters[8,9] indicates that ingredients closely related with the crystalline environment must be taken into account. This connection can be further explored by direct investigations of the sensitivity of the electronic structure on small deviations of the crystalline environment, as well as of the influence of such an environment on the nature and magnitude of the spin structures and the fluctuations that presumably mediate the superconductivity. In line with the second approach, the magnetic structures below T_N were resolved for a number of compounds, revealing interesting trends. The cubic CeIn$_3$ (Refs. 10 and 11) and tetragonal Ce$_2$RhIn$_8$ (Ref. 12) show commensurate magnetic structures with antiferromagnetic (AFM) alignment of Ce spins along the three nearest-neighbor directions (here called G-AFM phase in analogy to the nomenclature used in the manganites[13]), and CeRhIn$_5$ forms an incommensurate spiral along the $\vec{c}$ direction while still keeping the AFM coupling in the ab plane.[14,15] Recently, coexisting magnetic orders were

observed in the alloy system CeRh$_{1-x}$Ir$_x$In$_5$ in the interval $0.25 \lesssim x \lesssim 0.6$ where AFM and superconducting phases overlap.[16] The first AFM phase is identical to the spiral phase of CeRhIn$_5$, while the second one shows AFM alignment along the three nearest-neighbor directions such as in CeIn$_3$ (Refs. 10 and 11) and Ce$_2$RhIn$_8$.[12] These results indicate that distinct AFM ground states compete in this system, and that such competion may favor or be related with superconductivity.

Magnetic phenomena and their connection to crystal structures can be further explored by a thorough investigation of other members of the $R_m(\mathrm{Co,Rh,Ir})_n\mathrm{In}_{3m+2n}$ family (R=rare earth $\neq$ Ce, $n=0,1$; $m=1,2$). Since such compounds are not heavy fermions and/or superconductors, the knowledge thus obtained may be taken as a starting point to understand the more complex and rich behavior of the Ce-based compounds. Previous macroscopic studies on the $R_m(\mathrm{Co,Rh,Ir})_n\mathrm{In}_{3m+2n}$ family (R=Pr, Nd, Sm, Gd, and Tb) indicate that the evolution of the Néel temperature (T_N) with R does not follow the de Gennes scaling,[17,18] suggesting that crystal field or other anisotropy effects may be important to determine the critical temperatures and perhaps even the magnetic ground state in this system. Neutron scattering studies on NdIn$_3$ indicate a ground state with AFM alignment along two nearest-neighbor directions and FM alignment along the third direction, the C-AFM structure.[19] Additional phases with modulated moments along the FM directions have also been identified below the Néel temperature for this compound.[19,20] Similar C-AFM ground states

have been identified in NdRhIn$_5$ (Ref. [21]), Gd$_2$IrIn$_8$ (Ref. [22]), and TbRhIn$_5$.[23]

In continuation of the attempt to build a minimum comprehension of the magnetism of a spin-only system ($L=0$) under similar crystal environments to Ce$_m$(Co,Rh,Ir)$_n$In$_{3m+2n}$ ($n=0,1$; $m=1,2$) heavy-fermion superconductors, we carried out an experimental and theoretical investigation of the magnetic structure and fluctuations of a GdRhIn$_5$ single crystal. We note that the magnetism of Gd-based compounds is expected to be particularly simple, due to the absence of large orbital moments and crystal-field interactions associated with a half-filled $4f^7$ shell. The magnetic structure resolved here is of the C-AFM type, with partly frustrated first-neighbor (J_1) spin interactions. Based on this result and previous studies on other members of the R_m(Co,Rh,Ir)$_n$In$_{3m+2n}$ family, we conclude that the relative orientation between neighboring R-spins is determined primarily from a close competition between first- (J_1) and second-nearest-neighbor (J_2) AFM exchange interactions. This may be an important factor behind the complex magnetic behavior of the Ce-based compounds. The critical behavior close to the magnetic ordering transition in GdRhIn$_5$ was also investigated. The magnetic order parameter shows a power-law behavior close to the Néel temperature, characteristic of a second-order transition such as in Gd$_2$IrIn$_8$.[22] A theoretical renormalization group analysis was performed. Our results suggest that spin anisotropy terms, possibly arising from dipolar and other fairly weak interactions, must be claimed to understand the second order of the paramagnetic transition of GdRhIn$_5$ and the related compound Gd$_2$IrIn$_8$.

II. EXPERIMENTAL DETAILS

A single crystal of GdRhIn$_5$ was grown by the In-flux method as described previously.[17,24] The studied surface was finely polished with Al$_2$O$_3$ powder, yielding a single-peaked mosaic structure of $\sim$0.02° full width at half maximum (FWHM). The x-ray diffraction measurements were performed on the XRD2 beamline, placed after a dipolar source of the Laboratório Nacional de Luz Síncrotron, Campinas, Brazil.[25] The sample was mounted on the cold finger of a commercial closed-cycle He cryostat with a cylindrical Be window. The cryostat was fixed onto the Eulerian cradle of a commercial 4+2 circle diffractometer, appropriate for single crystal x-ray diffraction studies. The energy of the incident photons was selected by a double-bounce Si(111) monochromator, with water-refrigeration in the first crystal, while the second crystal was bent for sagittal focusing. The beam was vertically focused by a bent Rh-coated mirror placed before the monochromator, which also provided filtering of high-energy photons (third and higher order harmonics). A vertically focused beam was used in our measurements, delivering, at 7.24 keV, a flux of 3×10^{10} photons/s at 100 mA in a spot of $\sim$0.6 mm (vertical) $\times$2.0 mm (horizontal) at the sample, with an energy resolution of $\sim$5 eV. Our experiments were performed in the vertical scattering plane, i.e., perpendicular to the linear polarization of the incident photons. In most measurements, a solid state detector was used, except in the polarization study, in which a scintillation de-
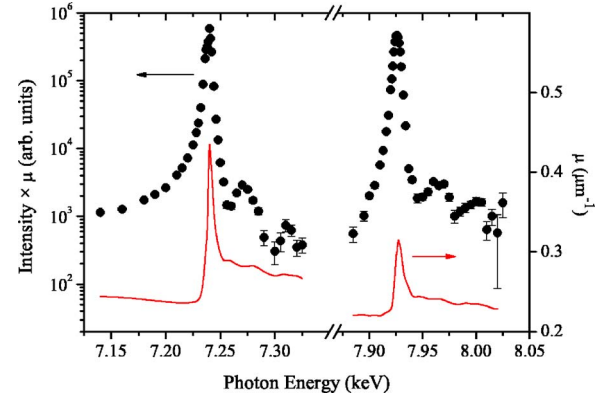

FIG. 1. (Color online) Energy-dependence of the integrated intensity of the $(0,\frac{1}{2},\frac{7}{2})$ Bragg reflection (symbols) across the Gd L_{III} and L_{II} edges. Data were corrected by the absorption coefficient μ obtained from the fluorescence yield (solid lines).

tector was placed after a Ge(111/333) analyzer crystal. At the energy corresponding to the Gd L_{II} edge, the analyzer placed at the Ge(333) reflection selects ($\sigma\rightarrow\sigma'$) scattering from the sample (i.e., scattered photons with the same polarization as the incident photons), while Ge(111) does not significantly discriminate the photon polarization [($\sigma\rightarrow\sigma'$) $+(\sigma\rightarrow\pi')$ channel].

III. MAGNETICALLY ORDERED PHASE

A. Polarization and resonance properties

Above $\sim$39 K, all the observed Bragg peaks were consistent with tetragonal symmetry of GdRhIn$_5$ (space group $P4/mmm$), without any detectable magnetic contribution. Below T_N=39 K, additional (h,k,l) Bragg reflections (h integer; k,l half-integers) were observed. Such reflections were dramatically enhanced at the Gd L_{II} and L_{III} edges (E=7.93 and 7.24 keV, respectively) due to resonance phenomena (see below). Polarization analysis at the Gd L_{III} edge using a Ge(111/333) analyzer crystal demonstrated pure ($\sigma\rightarrow\pi'$) scattering at these fractional positions at the reciprocal space, showing that such reflections are magnetic in origin, with dipolar resonances at this edge.[26,27]

The energy-dependence of the absorption-corrected intensity of the $(0,\frac{1}{2},\frac{7}{2})$ magnetic Bragg reflections at $\sim$12 K are shown in Fig. 1 around the Gd L_{III} and L_{II} edges (symbols). The energy-dependencies of the absorption coefficient, $\mu(E)$, obtained from fluorescence emission, are also given as solid lines. Resonant enhancements of over three orders of magnitude were observed at both edges. The intensity maximums occur $\sim$2 eV above the absorption edges, which were defined as the inflection points of $\mu(E)$. This result is consistent with a dominant dipolar nature ($2p\rightarrow5d$) of both resonances. Intensity oscillations of the $(0,\frac{1}{2},\frac{7}{2})$ magnetic peak were also observed above the edges, which we ascribe to a magnetic diffraction anomalous fine structure (DAFS).[28]

B. Magnetic structure

The positions in reciprocal space where magnetic Bragg reflections were observed lead to an AFM structure with

TABLE I. Comparison between observed and calculated intensities of magnetic Bragg reflections at 12 K, normalized by the most intense reflection, assuming the moments $\vec{m}$ along each one of the three axis of the unit cell. Experimental data were taken on resonance conditions, 2 eV above the Gd L_{II} edge.

(h,k,l)	I_{obs}	$\vec{m}\|\vec{a}$	$\vec{m}\|\vec{b}$	$\vec{m}\|\vec{c}$
$(0,-\frac{1}{2},\frac{7}{2})$	96(3)	100	11	21
$(0,\frac{1}{2},\frac{7}{2})$	100	100	11	21
$(0,-\frac{3}{2},\frac{7}{2})$	68(2)	93	100	21
$(0,\frac{3}{2},\frac{7}{2})$	68(2)	93	100	21
$(0,-\frac{1}{2},\frac{9}{2})$	99(2)	90	11	35
$(0,\frac{1}{2},\frac{9}{2})$	96(2)	90	11	35
$(0,-\frac{3}{2},\frac{9}{2})$	83(2)	83	100	35
$(0,\frac{3}{2},\frac{9}{2})$	79(2)	83	100	35
$(0,-\frac{1}{2},\frac{11}{2})$	95(2)	77	11	53
$(0,\frac{1}{2},\frac{11}{2})$	90(2)	77	11	53
$(1,-\frac{1}{2},\frac{11}{2})$	40(1)	41	21	100
$(1,\frac{1}{2},\frac{11}{2})$	43(1)	41	21	100

propagation vector $\vec{\tau}=(0,\frac{1}{2},\frac{1}{2})$. Since there is a single magnetic ion per chemical unit cell in the tetragonal structure of GdRhIn$_5$, the relative neighboring spin orientations are unequivocally determined from the $\vec{\tau}$-vector. According to this, linear ferromagnetic chains along the $\vec{a}$ direction are antiferromagnetically coupled along the other two axes (i.e., a C-type AFM structure). The direction of the magnetic moments may be obtained from the intensities of some magnetic Bragg peaks. The expression for such intensities shows a simple form in the present case for dipolar resonances and colinear magnetic structures, and is given by $I^M(\vec{\tau}) \propto (\vec{m}\cdot\vec{k}_s)^2$, where $\vec{m}$ is the magnetic moment, and $\vec{k}_s$ is the wave vector of the scattered light.[26,27] Comparisons of the observed intensities with calculated ones for the magnetic moments along $\vec{a}$, $\vec{b}$, and $\vec{c}$ directions are given in Table I. Good agreement between calculated and experimental data are obtained for the magnetic moments pointing towards the direction of the ferromagnetic chains, i.e., the $\vec{a}$ direction. Figure 2 displays the magnetic structure of GdRhIn$_5$, as determined above. This structure is consistent with a ^{155}Gd Mössbauer spectroscopy study in this compound, which indicated a colinear magnetic structure with the spins lying in the ab plane.[29]

C. Search for symmetry lowering of the crystal or electronic structure

It is interesting to note that the magnetic structure shown in Fig. 2 does not have a tetragonal symmetry, in the sense that the ferromagnetic chains are aligned along one specific direction in the ab plane, namely the $\vec{a}$ direction. It is therefore valid to ask whether a symmetry lowering of the crystal and/or electronic structure from the $P4/mmm$ space group also occurs, either by an orthorhombic distortion of the lattice parameters or by the presence of a charge density wave.
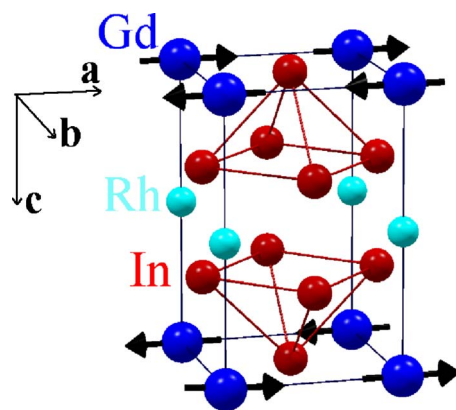

FIG. 2. (Color online) Magnetic structure of GdRhIn$_5$.

These possibilities were also investigated by synchrotron x-ray diffraction.

First, a hypothetical orthorhombic distortion was probed by measuring the Bragg interplane distances d_{hkl} of a set of $(00l)$, $(h0l)$, and $(0kl)$ charge reflections, using a monochromatic x-ray beam with energy $E=14\,472$ eV and resolution $(\delta E/E=1.0\times10^{-3})$. The irradiated (001) surface was the same used in the magnetic diffraction investigation. A scintillation detector was placed after a Si(111) analyzer crystal. We used the usual relation $d_{hkl}^2=1/[(h/a)^2+(k/b)^2+(l/c)^2]$ for orthogonal axes, obtaining the lattice parameter c directly from d_{00l}. The a and b parameters were then obtained from d_{h0l} and d_{0kl}. Table II shows the results at 20 and 300 K, indicating a metrically tetragonal phase within experimental errors. We should mention that the lattice metrics at intermediate temperatures were not investigated in the present work.

The possibility of an orthorhombic structure presenting a mosaic of domains with interchanged $\vec{a}$ and $\vec{b}$ axes was also considered. In this case, a two-peak structure is expected at each $(h0l)$ or $(0kl)$ reflection. Such a structure was not observed in our measurements, rather yielding single symmetric Lorentzian line shapes. In this case, the upper limit for the orthorhombic distortion is set by the measured peak widths. This information is also given in Table II in terms of $\delta\theta/\tan(\theta)$. A larger $\delta\theta/\tan(\theta)$ for $(h0l)$ and $(0kl)$ reflections with respect to $(00l)$ reflections would be consistent with an orthorhombic distortion or anisotropic strain in the ab plane. Nonetheless, it is seen that no additional broadening of the $(h0l)$ or $(0kl)$ peaks with respect to $(00l)$ was observed within our resolution. In addition, the peak widths are the same at 20 and 300 K, showing the absence of any temperature-dependent distortion or strain. Using the data of Table II, the upper limit of the hypothetical orthorhombic distortion is inferred to be $[(b-a)/a]\lesssim2\times10^{-4}$ for both single-domain or mosaic (multidomain) distortions. We conclude that no relevant bulk lattice distortion or anisotropic strain associated with the anisotropy of the magnetic structure along the $\vec{a}$ axis take place in this compound.

The possible presence of charge density waves (CDWs) was probed by a systematic search in reciprocal space at x-ray energies of 7930 eV (resonant condition at Gd L_{II} absorption edge) and at 7106.7 eV (below the Gd L_{III} absorption edge). A set of charge reflections—(001), (002), (011),

TABLE II. Extraction of the a, b, and c lattice parameters at 20 K and 300 K from selected $(00l)$, $(h0l)$, and $(0kl)$ Bragg peaks. The width of radial $(\theta-2\theta)$ scans are also given in terms of $\delta\theta/\tan(\theta)$ (full width at half maximum), where θ is the Bragg angle.

Miller indices	a, b, or c 20 K	$\delta\theta/\tan(\theta)$ (degrees) 20 K	a, b, or c 300 K	$\delta\theta/\tan(\theta)$ (degrees) 300 K
(006)	$c=7.4302(3)$ Å	0.0364(5)	$c=7.4479(4)$ Å	0.0367(6)
(004)	$c=7.4299(3)$ Å	0.0372(6)	$c=7.4473(4)$ Å	0.0377(6)
(308)	$a=4.5919(8)$ Å	0.0370(8)	$a=4.6066(8)$ Å	0.0378(9)
(207)	$a=4.5922(8)$ Å	0.0363(8)	$a=4.6059(8)$ Å	0.0369(8)
(044)	$b=4.5935(6)$ Å	0.0373(8)	$b=4.6078(6)$ Å	0.0386(8)
(043)	$b=4.5934(6)$ Å	0.0359(8)	$b=4.6081(6)$ Å	0.0376(8)

(022), (021), (102)—was chosen to define the borders of the one-dimensional scans in reciprocal space. Several scans along high symmetry h, k, and l mixed and unmixed directions were performed at $T=11.5$ K. The search was completed by two-dimensional hk, hl, and kl maps with a common border at the (022) reciprocal space position $(\delta h, \delta k, \delta l=0.5)$. We did not find any extra peak that might be assigned to previously unknown ordered structures. Although our scan procedure had been unable to directly reveal the existence of new electronic or structural phases in GdRhIn$_5$, we cannot completely rule out the possibility of the existence of low-symmetry incommensurate phases such as CDWs, since we did not investigate the whole reciprocal space volume.

D. Discussion: Rise of the *C*-AFM magnetic structure and competition with *G*-AFM: the role of long-range exchange interactions

In the $R_m(\text{Co},\text{Rh},\text{Ir})_n\text{In}_{3m+2n}$ (R=rare earth$\neq$Ce) family, the main coupling between the R ions comes from the Ruderman-Kittel-Kasuya-Yosida (RKKY) mechanism.[30] If we consider antiferromagnetic couplings only between the first-(J_1) and the second-nearest-neighbors (J_2), the magnetic ground state is determined by their relative strength $\alpha \equiv J_1/J_2$. The *G*-AFM structure represented in Fig. 3 frustrates J_2 but satisfies J_1 and would be favored by $\alpha \gg 1$. On the other hand, the *C*-AFM structure satisfies part of J_1 and
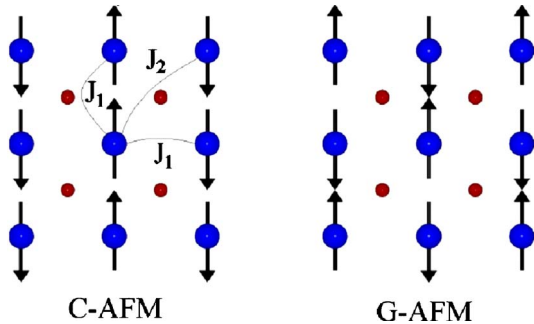

FIG. 3. (Color online) Two-dimensional representation of the *C*-AFM and *G*-AFM spin structures. The first- and second-nearest-neighbor exchange interactions (J_1 and J_2, respectively) are also indicated.

all J_2 interactions and thus may be favored if J_1 and J_2 are comparable in magnitude. For the RKKY interaction, α usually depends on the first- and second-neighbor distances among the rare-earth ions and on the topology of the Fermi surface of each compound. However, in these compounds the topology and volume of the Fermi surface depends little on the particular rare-earth ion since the localized $4f$ electrons do not hybridize considerably with the conduction band, with the possible exceptions of some Ce-based compounds. Also, we note that the tetragonal a-lattice parameter shows only small variations along the $R_m(\text{Co},\text{Rh},\text{Ir})_n\text{In}_{3m+2n}$ series $(\lesssim 2\%)$.[17] It is therefore not completely surprising that the magnetic structures of all known $R_m(\text{Co},\text{Rh},\text{Ir})_n\text{In}_{3m+2n}$ (R=Nd to Gd) compounds are similar, characterized by ferromagnetic chains along a specific first-nearest-neighbor direction $(\vec{a})$ with an AFM coupling along $\vec{b}$ and $\vec{c}$, i.e., the *C*-AFM structure (see Fig. 2 and Refs. 19–22).

The orientation of the magnetic moment in any of these magnetic structures is determined by anisotropic interactions. The direction of the staggered moment for GdRhIn$_5$ is in agreement with other tetragonal compounds with the same antiferromagnetic wave-vector and staggered moment direction, such as GdAu$_2$Si$_2$ (Ref. 31) and GdCu$_2$Si$_2$.[32] It has been argued that in these cases the magnetic dipolar interaction is the dominant source of anisotropy (being of the order of tens of μeV).[31] The same appear to hold for GdRhIn$_5$. Nonetheless, we should mention that other possible sources of anisotropy for Gd compounds, such as a spin-orbit coupling of the conduction electrons[33] or crystal electric field via excited states[34–37] might in principle be relevant to the problem.

The same general conclusions for the ground state may remain valid when the spin anisotropy due to the relevant crystal field effects is introduced in the Hamiltonian for $R \neq$ Gd. In this case, the crystal field effects determine the spin direction with respect to the unit cell axes and may affect T_N,[38] but the relative orientation between neighboring R-spins is still determined mainly by α.

The extension of the above scenario for the Ce-based compounds is not straightforward. This is because the Ce $4f$ electrons may be hybridized with the conduction band. In cases where the Ce $4f$ electrons are itinerant, the RKKY mechanism is no longer applicable. On the other hand, for compounds with localized $4f$ moments, the above scenario of J_1/J_2 competition might be useful. Particularly, deHaas

van Alphen measurements on $Ce_{1-x}La_xRhIn_5$ showed no significant change in the Fermi surface topology or volume over the entire doping range $(0<x<1)$,[39] showing that the $4f$ electrons remain localized. Thus, we focus our discussion on the magnetic structure of $CeRhIn_5$ with localized moments. This compound shows AFM alignment along two directions $(\vec{a}$ and $\vec{b})$, and a spiral alignment along the tetragonal $\vec{c}$ axis,[14] defining a propagation vector $\vec{\tau}=\left(\frac{1}{2},\frac{1}{2},0.297\right)$. This magnetic structure may be seen as an intermediate case between the G-AFM structure $\left(\vec{\tau}_1=\left(\frac{1}{2},\frac{1}{2},\frac{1}{2}\right)\right)$ and a C-AFM structure with the FM chains along the $\vec{c}$ direction $\left(\vec{\tau}_2=\left(\frac{1}{2},\frac{1}{2},0\right)\right)$. Notice that the C-AFM structure is expected to be a competitive ground state, since α is expected to be similar for $CeRhIn_5$ and $GdRhIn_5$ due to presumably similar Fermi surfaces. On the other hand, the G-AFM state also appears to be competitive for the Ce-based compounds, since it is the ground state of $CeIn_3$ (Refs. 10 and 11) and Ce_2RhIn_8.[12] It is therefore not implauable to infer that the incommensurate magnetic structure of $CeRhIn_5$ is actually a result of a close competition between the G-AFM and C-AFM ground states, paving the way for the stabilization of an intermediate spiral phase, perhaps with the aid of very long-range RKKY interactions (J_3, J_4, etc).

IV. CRITICAL BEHAVIOR

A. Experimental

The critical behavior of the sublattice magnetization at the paramagnetic transition was investigated. Figures 4(a) and 4(b) show the T dependence of the intensity of the $\left(0,\frac{1}{2},\frac{11}{2}\right)$ magnetic Bragg peak of $GdRhIn_5$ in different T intervals. Close to and below $T_N=39$ K, this could be fitted by a power-law behavior, $I\propto(1-T/T_N)^{2\beta}$, which is characteristic of a second-order transition. The experimental determination of the critical parameter β depends slightly on the temperature interval in which the fitting is performed. For fits in T intervals $(T_N-T)/T_N<0.01$, <0.03, and <0.05, one obtains $\beta=0.370(16)$, $0.346(5)$, and $0.339(4)$, respectively. Quoted errors in parentheses are statistical only, and represent one standard deviation. Figure 4(c) shows the T dependence of the width of the $\left(0,\frac{1}{2},\frac{11}{2}\right)$ magnetic peak, as obtained in radial $(\theta-2\theta)$ scans. Much below T_N, the width is instrumental only, indicating long-range order with correlation length above ~5000 Å. For $0.998T_N<T<T_N$, a peak broadening above the instrumental resolution was noticed. The inset of Fig. 4(c) displays the magnetic correlation length in this T interval, obtained from the peak broadening data. We should mention that, above T_N, the intensities were below our detection limit for this sample, thus the short-range dynamic correlations in the paramagnetic phase could not be investigated.

These results for $GdRhIn_5$ may be compared to the previously reported measurements for Gd_2IrIn_8, where a larger critical parameter $\beta=0.39$ was obtained for the critical interval $(T_N-T)/T_N<0.10$.[22] The comparison becomes clear in Fig. 4(b), where the critical behavior of Gd_2IrIn_8, using data of Ref. 22 is directly compared to $GdRhIn_5$. In the ordered
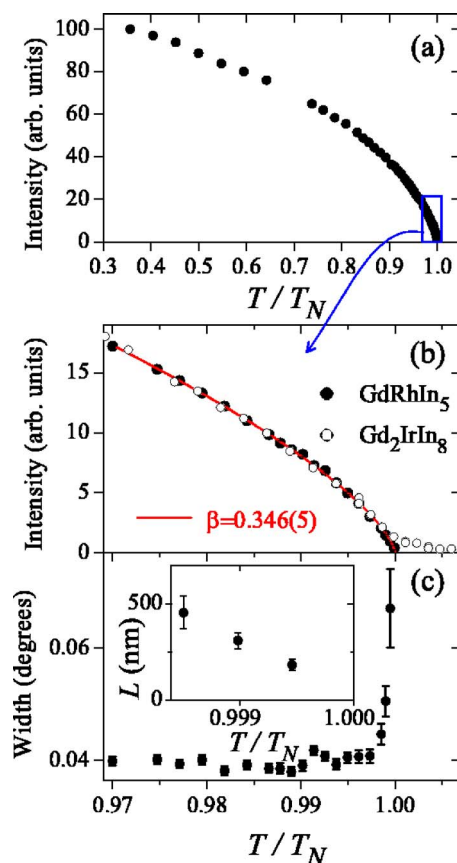

FIG. 4. (Color online) Temperature-dependence of the (a), (b) integrated intensity and (c) width of radial $(\theta-2\theta)$ scans of the $\left(0,\frac{1}{2},\frac{11}{2}\right)$ magnetic Bragg reflection of $GdRhIn_5$ and $\left(\frac{1}{2},0,4\right)$ reflection of Gd_2IrIn_8 (taken from Ref. 22). A fit to a critical power law behavior, $(T_N-T)^{2\beta}$, characteristic of a second-order transition, is given in (b) as a line. The inset shows the correlation length L, obtained from the data in (c) after deconvolution of the instrumental width. The experiment was performed in resonance conditions, 2 eV above the Gd L_{II}-edge.

phase ($T<T_N$), both compounds appear to show identical behavior, described by the same critical exponent $\beta\sim0.35$. However, while the magnetic intensities tend to zero as $T\sim T_N$ for $GdRhIn_5$, a significant residual scattering was observed near and above the transition for Gd_2IrIn_8, which may be mostly ascribed to persistent magnetic order or correlations in the near surface region.[22,40] This effect smooths out the transition observed by x-ray diffraction, and interferes severely in the extraction of the β critical exponent. We conclude that, although both compounds were equally finely polished before measurements, the Gd_2IrIn_8 surface showed this effect in a larger degree, leading to a less reliable extraction of the β exponent. Perhaps the most relevant information from this analysis is that a direct comparison of the magnetic intensities of Gd_2IrIn_8 and $GdRhIn_5$ near T_N reveals an identical behavior in the T interval where the surface effects are negligible, consistent with an identical critical exponent $\beta\sim0.35$. This conclusion is in agreement with the prediction that both compounds belong to the same universality class for magnetism (see below).

B. Renormalization group analysis

The experimental critical behavior described above may be compared with theoretical expectations based on the symmetry of the crystal and magnetic structures of this compound. As demonstrated by Muckamel *et al.*,[41,42] the Ginzburg-Landau-Wilson (GLW) Hamiltonian for the class of antiferromagnetic problems is written in terms of a staggered order parameter (OP) with a total number of components $N = nm$, where n is the number of spin components allowed by the irreducible representations of the paramagnetic space group, or equivalently, the number of degrees of freedom for the critical spin fluctuations, and m is the number of ways the unitary cell may be enlarged by all distinct AFM ordering wave vectors allowed by the symmetry of the crystal. The total number of components may easily exceed $N \geq 4$,[43] opening up the possibility to classical fluctuation-induced first-order transitions, such as those already reported experimentally.[41,42] The criterion for the study of phase transitions using renormalization group (RG) theoretical methods is based on the stability of the fixed points in the RG flow, in the sense that the phase transition is of second order when the flow continuously approaches a fixed point which is stable with respect to the fluctuations of the staggered field, and indicates something else like an abrupt or a smeared transition otherwise, when the flow exhibits a runaway.[44]

Because of the critical exponents universality, the phase transition is sensitive only to a few parameters like the dimension d of the system, the number of components N of the OP and the symmetry of the crystal, which reflects in the anisotropies of the Hamiltonian. As shown by Brézin *et al.*,[43] for $N \geq 4$, the isotropic fixed point is always unstable with respect to anisotropies in the original Hamiltonian, while for $N < 4$ this fixed point is always stable because the O(N) symmetry is dynamically generated near the critical point.

Here, we concentrate the analysis on a few compounds of the $Gd_m(Rh, Ir)_n In_{3m+2n}$ series, including the title compound. In the cubic $GdIn_3$ crystal, the observed AFM propagation vector $\vec{\tau} = (\frac{1}{2}, \frac{1}{2}, 0)$[46] represents an ordering state which is degenerated with the states represented by the propagation vectors $(0, \frac{1}{2}, \frac{1}{2})$ and $(\frac{1}{2}, 0, \frac{1}{2})$, resulting in $m = 3$ distinct AFM propagation vectors allowed by the crystal symmetry. Since $n \leq 3$ is the total number of spin degrees of freedom, the staggered OP of $GdIn_3$ has a total number of $N = 3n \leq 9$ components. In the tetragonal Gd_2IrIn_8 crystal, the cubic symmetry is broken in the [001] direction by nonmagnetic planes of Ir.[22] This crystal orders antiferromagnetically along the $\vec{\tau} = (\frac{1}{2}, 0, 0)$ direction, which is equivalent by symmetry to the $(0, \frac{1}{2}, 0)$ direction, giving $m = 2$ and $N = 2n \leq 6$ OP components. Since the magnetization of $GdRhIn_5$ orders along the $\vec{\tau} = (0, \frac{1}{2}, \frac{1}{2})$ direction (which is equivalent by symmetry to the $(\frac{1}{2}, 0, \frac{1}{2})$ direction), its staggered OP has the same number of components of Gd_2IrIn_8, $N = 2n \leq 6$.

In isotropic magnetic systems, the equality $n = 3$ holds for the number of spin degrees of freedom, and all of the above relations for N are valid with the equality sign. As we will show below, the renormalization group results indicate that if $GdRhIn_5$, Gd_2IrIn_8, and $GdIn_3$ were perfectly isotropic spin systems, first-order transitions would be obtained for all three compounds,[43] in contrast with the second-order transitions observed for $GdRhIn_5$ (see Fig. 4) and Gd_2IrIn_8 (see Ref. 22). We conclude that spin anisotropy must be properly taken into account for a correct analysis of the critical behavior or these compounds. As noted in Sec. III D, a number of distinct possible sources of anisotropy may be anticipated for Gd compounds with half-filled $4f^7$ shell, such as dipolar interactions,[31] spin-orbit coupling of the conduction electrons[33] or crystal electric field via excited states.[34–37] The strength of such interactions is typically of the order of tens of μeV.[31,33] Even though this energy scale is about three orders of magnitude weaker than typical exchange energies in Gd systems, we note, for example, that there are consistent evidences that in Gd metal the dipolar interaction is not only responsible for the ground state anysotropy but also determines its critical behavior.[48,49]

In order to proceed with our analysis, the major source of anisotropy must be identified. Since there are recent indications that dipolar interactions are the major source of anisotropy[31] and responsible for the specific heat behavior in an extensive variety of Gd compounds,[45,50,51] we pay attention to the possible influence of the dipolar coupling in the critical behavior of these materials. The dipolar anisotropy breaks the rotational symmetry of the Gd spins by lowering the size of the space of degenerated states where the spins are allowed to fluctuate. In the RG sense, the influence of the dipolar interaction will be decisive if it proves to be a relevant source of anisotropy in a previously isotropic Hamiltonian.[47] The difficulty of the RG method here is that it leads to rather inconclusive results when the RG flow has no stable fixed points, since the flow rapidly moves toward a region where the technique is no longer valid. To see this, we write down the most general classical Hamiltonian that describes the physics of the isotropic Gd spin problem, which corresponds to a GLW Hamiltonian of m coupled O(n) symmetric models,

$$H_0(\phi) = \int d^d x \left\{ \frac{1}{2} \sum_{\alpha,i} [r_0 \phi_{\alpha i}^2 + (\nabla \phi_{\alpha i})^2] + u \sum_{\alpha,i,j} \phi_{\alpha i}^2 \phi_{\alpha j}^2 \right.$$
$$\left. + v \sum_{\alpha \neq \beta} \sum_{ij} \phi_{\alpha i}^2 \phi_{\beta j}^2 + w \sum_{\alpha \neq \beta} \sum_{ij} \phi_{\alpha i} \phi_{\beta i} \phi_{\alpha j} \phi_{\beta j} \right\},$$
$$(1)$$

where $\alpha, \beta = 1, \dots, m$ indexes the distinct AF wave vectors and $i, j = 1, \dots n \leq d$ labels the spin components in a given orthogonal basis, like x, y, z. Note that all terms are written as powers of scalar products of the spin components $\vec{\phi}_\mu \cdot \vec{\phi}_\nu$ because of the assumed rotational symmetry of the spins near the phase transition. The quartic terms differ only by the different ways to combine the Greek indexes that label the equivalent AF wave vectors. This Hamiltonian has a stable isotropic fixed point for $N = nm < 4$, which would lead to a second order phase transition, but no stable fixed points were found for $N > 4$, in agreement with the analysis of Ref. 52. Including a general dipolar interaction term, which in the antiferromagnetic case has the form (Ref. 47)

$$H_D = \int d^d x \sum_{\alpha i} \left[(\boldsymbol{\nabla}\phi_{i\alpha})^2 - f(\partial_i \phi_{i\alpha})^2 + h \sum_j \partial_i \phi_{i\alpha} \partial_j \phi_{j\alpha} \right],$$

$$(2)$$

where f and h are proportional to the dipolar coupling constant $(g\mu_B)^2$, with $g\mu_B$ being the total magnetic moment of the Gd ion, our RG flow suggests that the total Hamiltonian

$$H = H_0 + H_D \qquad (3)$$

preserves the same fixed points of the isotropic spin problem for $n=d$ (see Appendix A for details). In particular, the scaling of the dipolar parameters from equation

$$\frac{df}{dl} = -\eta_f f, \quad \frac{dh}{dl} = -\eta_h h, \qquad (4)$$

with

$$\eta_f = \eta_h = \frac{32}{3}\left(\frac{1}{8\pi^2}\right)^2 (2u^2 + (m-1)(v^2 + w^2)) \geqslant 0,$$

indicates that the dipolar interaction is irrelevant in the vicinity of the isotropic fixed point for $N<4$ ($n=d$), which corresponds to the case $m=1$. For larger m, however, ($m=2$ for GdRhIn$_5$, Gd$_2$IrIn$_8$, and $m=3$ for GdIn$_3$), we have not identified stable fixed points for the total Hamiltonian $H_0 + H_D$ ($n=d$) and although this would point to the direction of a fluctuation induced first order transition, as in the isotropic model, it is not clear what happens in this case. The fact that the f and h parameters flow initially to zero is expected, since we do not include sources of anisotropy in the bare Hamiltonian as the cubic term (v) from Ref. 47. Nevertheless, as pointed out in this reference, such terms could well be self generated in a higher loop expansion.

If we assume that dipolar interaction is relevant at the phase transition, it must break the spin rotational invariance of Hamiltonian (1). Once this symmetry is broken, the quartic terms should be written in the most general way allowed by the crystallographic group. In the particular case of the Gd series compounds we have studied, we have not identified bicritical, tricritical or multicritical points associated to the paramagnetic phase transition, meaning that the spin fluctuations are confined inside subspaces of degenerated spin configurations. In other words, each of these subspaces in the spin space correspond to an irreducible representation of the AF order parameter. The number and size of all the irreducible representations allowed follows directly from the crystallographic point group symmetry and from the position of the ordering wave-vector $\vec{\tau}$ in the Brillouin zone (BZ). In the case of GdRhIn$_5$, the $P4/mmm$ space group associated with the special point $\vec{\tau}=\left(\frac{1}{2},0,\frac{1}{2}\right)$, at the border of the BZ, has three irreducible representations of dimension m, with the spin pointing along the unit-cell axes of the crystal (for details, see Appendix B). In this case, the number of spin degrees of freedom for each representation is just $n=1$. The most general Hamiltonian would be

$$H = \int d^d x \left\{ \frac{1}{2}\sum_\alpha [r_0 \phi_\alpha^2 + c(\boldsymbol{\nabla}\phi_\alpha)^2] \right.$$
$$\left. + u\sum_\alpha \phi_\alpha^2 \phi_\alpha^2 + v\sum_{\alpha\neq\beta} \phi_\alpha^2 \phi_\beta^2 \right\}, \qquad (5)$$

with the dipolar interaction in this case simply renormalizing the gradient term. For $m=2$, as in the case of GdRhIn$_5$, this Hamiltonian has one $O(m)$ symmetric fixed point[43] with $\beta =0.36$ in two-loop expansion. The ordering wave vector $\vec{\tau} =\left(\frac{1}{2},0,0\right)$ of Gd$_2$IrIn$_8$ (also from space group $P4/mmm$) gives the same three irreducible representations of dimension m, and therefore GdRhIn$_5$ and Gd$_2$IrIn$_8$ both lie in the same universality class. In GdIn$_3$, the $Pm3m$ group acting on a BZ with the ordering wave-vector $\vec{\tau}=\left(\frac{1}{2},\frac{1}{2},0\right)$ admits one irreducible representation of size $N=m$, with the spin pointing along the $\vec{c}$ axis, and another one of size $N=2m$ with the spins confined in the ab plane. The Hamiltonian of the first representation follows the general form of Eq. (5), showing one isotropic fixed point for $m<4$. The second representation is larger ($N=6$) and its Hamiltonian follows Eq. (3), where no stable fixed points were found for $N>4$, which would indicate the possibility of a fluctuation-induced first-order transition for this case, even if the anisotropy is included. The magnetic phase transition of GdIn3 is currently under study and will be the subject of a more detailed analysis soon.

V. CONCLUSIONS

In summary, our resonant x-ray diffraction experiments show a C-AFM magnetic structure for GdRhIn$_5$ with the spins lying along the FM chain direction. This structure is rationalized in terms of a competition between first- and second-neighbors exchange interactions. This scenario was extended to other members of the $R_m(\text{Co},\text{Rh},\text{Ir})_n\text{In}_{3m+2n}$ (R =rare earth) family, in particular the Ce-based heavy-fermion superconductors. The critical behavior close to the paramagnetic transition was investigated, revealing a second-order transition with critical exponent $\beta\sim 0.35$ for GdRhIn$_5$ and Gd$_2$IrIn$_8$. A renormalization group analysis predicts that both compounds belong to the same universality class, in agreement with experiment. However, a first-order transition is predicted in the absence of spin anisotropy terms in the Hamiltonian, in contrast to our results, indicating that such terms may be important to stabilize a critical point in this family. Indeed, we show that if relevant dipolar interactions are assumed, then the renormalization group analysis predicts a second order phase transition for GdRhIn$_5$ and GdIr$_2$In$_8$ with $\beta=0.36$ in two-loop ϵ expansion, in good agreement with our experiments.

APPENDIX A: RG PROCEDURE

Since the dipolar interaction is marginally relevant at the one loop level, the RG calculation has to go to a second loop expansion. Following the standard RG procedure along the lines of Ref. 48 for $n=d=4-\epsilon$, where ϵ is the perturbative parameter of the expansion (which we set to $\epsilon=1$ in the end),

we integrate out of the partition function the fluctuation modes with wave-vectors $b^{-1} < |\mathbf{k}| < 1$ (which we denote by $\int_> dk$ and $b \gg 1$) and rescale the spins. This leads to a renormalization of the dipolar part of the Hamiltonian (2) according to

$$\Gamma_2(\mathbf{q}) = -16(2u^2 + (m-1)(v^2 + w^2))$$

$$\times \int_> d\mathbf{k} \, G_{ij}(\mathbf{k}) \sum_{lm} I_{lmm}(\mathbf{k} - \mathbf{q})$$

$$-32(2u^2 + (m-1)vw)$$

$$\times \int_> d\mathbf{k} \sum_m G_{im}(\mathbf{k}) \sum_l I_{lmj}(\mathbf{k} - \mathbf{q}), \qquad \text{(A1)}$$

where

$$I_{\gamma\delta\beta}(\mathbf{p}) = \int_> d^d\mathbf{k} \, G_{\gamma\delta}(\mathbf{k}) G_{\gamma\beta}(\mathbf{k} + \mathbf{p}).$$

We assume that the dipolar interaction is strong enough in the critical region, i.e., $T - T_c \ll \frac{(g\mu_B)^2}{a^3}$, so that the bare propagator is given by

$$G_{ij}(\mathbf{k}) = \frac{1}{k^2}\left[\delta_{ij} - h_0 \frac{k_i k_j}{k^2} + f_0 \left(\frac{k_i}{k}\right)^2 \delta_{ij} \right],$$

with f_0 and h_0 being proportional to the dipolar coupling constant and to geometric factors reflecting the lattice symmetry [see Eq. (23) from Ref. 47]. After performing the integrals on Eq. (A1) and expanding $\Gamma_2(\mathbf{q})$ to second order in $\mathbf{q}$, which though rather cumbersome is straightforward, we obtain Eq. (4). Since f and h flow initially to zero, the available fixed points up to this order correspond to the fixed points of the isotropic Hamiltonian (1). The RG of the isotropic problem has been studied in detail by Ref. 52, which indicates the absence of stable fixed points for $N = nm > 4$. The absence of stable fixed points within the isotropic model remains inaltered with the inclusion of long-range correlated quenched disorder.[53] In one-loop at least, the disordered isotropic model produces no new stable fixed points[54] beyond the two unphysical fixed points previously found by Halpering and Weinrib.[53]

APPENDIX B: IRREDUCIBLE REPRESENTATIONS OF GdRhIn5

The simplest way to obtain all the irreducible representations allowed by the crystallographic point group for a given ordering point $\vec{\tau}$ in the BZ is to decompose the spins in a given basis *fixed* with respect to $\vec{\tau}$, and then apply all the point group symmetry operations to see how the spin components in the original basis will change. The idea is that if we properly choose the original spin basis, then we are able to identify the subspaces where the spins will be confined by the application of the symmetry operations allowed by the crystal point group only. For GdRhIn5, which ordering wave vectors are

$$\vec{\tau}_{\alpha=1} = \left(\frac{1}{2}, 0, \frac{1}{2}\right),$$

$$\vec{\tau}_{\alpha=2} = \left(0, \frac{1}{2}, \frac{1}{2}\right),$$

we will define the spin basis by $\{\vec{\nu}_{1,\alpha}, \vec{\nu}_{2,\alpha}\vec{\nu}_{3,\alpha}\}$, where

$$\vec{\nu}_{1,\alpha=1} = (1,0,0),$$

$$\vec{\nu}_{2,\alpha=1} = (0,1,0),$$

$$\vec{\nu}_{3,\alpha=1} = (0,0,1),$$

$$\vec{\nu}_{1,\alpha=2} = (0,1,0),$$

$$\vec{\nu}_{2,\alpha=2} = (-1,0,0),$$

$$\vec{\nu}_{3,\alpha=2} = (0,0,1).$$

Denoting $\phi_{i,\alpha}$ as $\phi_{i,1} = \phi_i$ and $\phi_{i,2} = \bar{\phi}_i$ for the ith spin component with respect to the αth ordering wave vector, the symmetry operations of the $P4/mmm$ point group generators are

$$C_4[001]: \phi_1 \leftrightarrow \bar{\phi}_1, \quad \phi_2 \leftrightarrow \bar{\phi}_2, \quad \phi_3 \rightarrow \bar{\phi}_3 \rightarrow -\phi_3,$$

$$C_2[100]: \phi_1 \rightarrow -\phi_1, \quad \phi_2 \rightarrow \phi_2, \quad \phi_3 \rightarrow \phi_3,$$

$$\bar{\phi}_1 \rightarrow -\bar{\phi}_1, \quad \bar{\phi}_2 \rightarrow \bar{\phi}_2, \quad \bar{\phi}_3 \rightarrow -\bar{\phi}_3,$$

$$i: \phi_j \rightarrow -\phi_j, \quad \bar{\phi}_j \rightarrow -\bar{\phi}_j.$$

We see that once a spin points along one of the i directions (which are fixed with respect to $\vec{\tau}_\alpha$) the application of the crystallographic point group symmetry operations will "trap" it on the same i direction of the "rotated" α basis, and therefore, the spin space for each representation is one dimensional. This results in three irreducible representations of size $N = m = 2$.

---

[1] H. Hegger, C. Petrovic, E. G. Moshopoulou, M. F. Hundley, J. L. Sarrao, Z. Fisk, and J. D Thompson, Phys. Rev. Lett. **84**, 4986 (2000).

[2] C. Petrovic, P. G. Pagliuso, M. F. Hundley, R. Movshovich, J. L. Sarrao, J. D. Thompson, Z. Fisk, and P. Monthoux, J. Phys.: Condens. Matter **13**, L337 (2001).

[3] C. Petrovic, R. Movshovich, M. Jaime, P. G. Pagliuso, M. F.

Hundley, J. L. Sarrao, Z. Fisk, and J. D. Thompson, Europhys. Lett. **53**, 254 (2001).

[4] P. G. Pagliuso, C. Petrovic, R. Movshovich, D. Hall, M. F. Hundley, J. L. Sarrao, J. D. Thompson, and Z. Fisk, Phys. Rev. B **64**, 100503(R) (2001).

[5] J. D. Thompson, R. Movshovich, Z. Fisk, F. Bouquet, N. J. Curro, R. A. Fisher, P. C. Hammel, H. Hegger, M. F. Hundley, M. Jaime, P. G. Pagliuso, C. Petrovic, N. E. Phillips, and J. L. Sarrao, J. Magn. Magn. Mater. **226**, 5 (2001).

[6] T. Moriya and K. Ueda, Rep. Prog. Phys. **66**, 1299 (2003).

[7] J. D. Thompson, M. Nicklas, A. Bianchi, R. Movshovich, A. Llobet, W. Bao, A. Malinowski, M. F. Hundley, N. O. Moreno, P. G. Pagliuso, J. L. Sarrao, S. Nakatsuji, Z. Fisk, R. Borth, E. Lengyel, N. Oeschler, G. Sparn, and F. Steglich, Physica B **329-333**, 446 (2003).

[8] P. G. Pagliuso, R. Movshovich, A. D. Bianchi, M. Nicklas, J. D. Thompson, M. F. Hundley, J. L. Sarrao, and Z. Fisk, Physica B **312-313**, 129 (2002).

[9] E. D. Bauer, J. D. Thompson, J. L. Sarrao, L. A. Morales, F. Wastin, J. Rebizant, J. C. Griveau, P. Javorsky, P. Boulet, E. Colineau, G. H. Lander, and G. R. Stewart, Phys. Rev. Lett. **93**, 147005 (2004).

[10] A. Benoit, J. X. Boucherle, P. Convert, J. Flouquet, J. Palleau, and J. Schweizer, Solid State Commun. **34**, 293 (1980).

[11] J. M. Lawrence and S. M. Shapiro, Phys. Rev. B **22**, 4379 (1980).

[12] W. Bao, P. G. Pagliuso, J. L. Sarrao, J. D. Thompson, Z. Fisk, and J. W. Lynn, Phys. Rev. B **64**, 020401(R) (2001).

[13] E. O. Wollan and W. C. Koehler, Phys. Rev. **100**, 545 (1955).

[14] W. Bao, P. G. Pagliuso, J. L. Sarrao, J. D. Thompson, Z. Fisk, J. W. Lynn, and R. W. Erwin, Phys. Rev. B **62**, R14621 (2000); **63**, 219901(E) (2001); **67**, 099903(E) (2003).

[15] N. J. Curro, P. C. Hammel, P. G. Pagliuso, J. L. Sarrao, J. D. Thompson, and Z. Fisk, Phys. Rev. B **62**, R6100 (2000).

[16] A. D. Christianson, A. Llobet, W. Bao, J. S. Gardner, I. P. Swainson, J. W. Lynn, J.-M. Mignot, K. Prokes, P. G. Pagliuso, N. O. Moreno, J. L. Sarrao, J. D. Thompson, and A. H. Lacerda, Phys. Rev. Lett. **95**, 217002 (2005).

[17] P. G. Pagliuso, J. D. Thompson, M. F. Hundley, J. L. Sarrao, and Z. Fisk, Phys. Rev. B **63**, 054426 (2001).

[18] R. Lora-Serrano, L. Mendonça-Ferreira, D. J. Garcia, E. Miranda, C. Giles, J. G. S. Duque, E. Granado, and P. G. Pagliuso, Physica B **384**, 326 (2006).

[19] S. Mitsuda, P. M. Gehring, G. Shirane, H. Yoshizawa, and Y. Onuki, J. Phys. Soc. Jpn. **61**, 1469 (1992).

[20] M. Amara, R. M. Galéra, P. Morin, T. Veres, and P. Burlet, J. Magn. Magn. Mater. **130**, 127 (1994); M. Amara, R. M. Galéra, P. Morin, J. Voiron, and P. Burlet, *ibid.* **131**, 402 (1994).

[21] S. Chang, P. G. Pagliuso, W. Bao, J. S. Gardner, I. P. Swainson, J. L. Sarrao, and H. Nakotte, Phys. Rev. B **66**, 132417 (2002).

[22] E. Granado, P. G. Pagliuso, C. Giles, R. Lora-Serrano, F. Yokaichiya, and J. L. Sarrao, Phys. Rev. B **69**, 144411 (2004).

[23] R. Lora-Serrano, C. Giles, E. Granado, D. J. Garcia, E. Miranda, O. Agüero, L. Mendonça-Ferreira, J. G. S. Duque, and P. G. Pagliuso, Phys. Rev. B **74**, 214404 (2006).

[24] Z. Fisk and J. P. Remeika, in *Handbook on the Physics and Chemistry of Rare Earths*, edited by J. K. A. Gschneider and E. L. Eyring (Elsevier, North-Holland, 1989), Vol. 12, p. 53.

[25] C. Giles, F. Yokaichiya, S. W. Kycia, L. C. Sampaio, D. C. Ardiles-Saravia, M. K. K. Franco, and R. T. Neuenschwander, J.

[—] Synchrotron Radiat. **10**, 430 (2003).

[26] J. P. Hill and D. F. McMorrow, Acta Crystallogr., Sect. A: Found. Crystallogr. **52**, 236 (1996).

[27] S. W. Lovesey and S. P. Collings, in *X-Ray Scattering and Absorption by Magnetic Materials* (Oxford Science Publications, Oxford, 1996).

[28] H. Stragier, J. O. Cross, J. J. Rehr, L. B. Sorensen, C. E. Bouldin, and J. C. Woicik, Phys. Rev. Lett. **69**, 3064 (1992).

[29] K. Latka, R. Kmieć, M. Rams, A. W. Pacyna, V. I. Zaremba, and R. Pöttgen, Z. Naturforsch., B: Chem. Sci. **59**, 947 (2004).

[30] M. A. Ruderman and C. Kittel, Phys. Rev. **96**, 99 (1954); T. Kasuya, Prog. Theor. Phys. **16**, 45 (1956); K. Yosida, Phys. Rev. **106**, 893 (1957).

[31] M. Rotter, M. Loewenhaupt, M. Doerr, A. Lindbaum, H. Sassik, K. Ziebeck, and B. Beuneu, Phys. Rev. B **68**, 144418 (2003).

[32] J. M. Barandiaran, D. Gignoux, D. Schmitt, J. C. Gomez-Sal, J. Rodriguez Fernandez, P. Chieux, and J. Schweizer, J. Magn. Magn. Mater. **73**, 233 (1988).

[33] M. Colarieti-Tosti, S. I. Simak, R. Ahuja, L. Nordström, O. Eriksson, D. Aberg, S. Edvardsson, and M. S. S. Brooks, Phys. Rev. Lett. **91**, 157201 (2003).

[34] B. G. Wybourne, Phys. Rev. **148**, 317 (1966).

[35] S. E. Barnes, Phys. Rev. B **9**, 4789 (1974).

[36] S. E. Barnes, K. Baberschke, and M. Hardiman, Phys. Rev. B **18**, 2409 (1978).

[37] R. R. Urbano, C. Rettori, G. E. Barberis, M. Torelli, A. Bianchi, Z. Fisk, P. G. Pagliuso, A. Malinowski, M. F. Hundley, J. L. Sarrao, and S. B. Oseroff, Phys. Rev. B **65**, 180407(R) (2002).

[38] P. G. Pagliuso, D. J. Garcia, E. Miranda, E. Granado, R. Lora Serrano, C. Giles, J. G. S. Duque, R. R. Urbano, C. Rettori, J. D. Thompson, M. F. Hundley, and J. L. Sarrao, J. Appl. Phys. **99**, 08P703 (2006).

[39] U. Alver, R. G. Goodrich, N. Harrison, D. W. Hall, E. C. Palm, T. P. Murphy, S. W. Tozer, P. G. Pagliuso, N. O. Moreno, J. L. Sarrao, and Z. Fisk, Phys. Rev. B **64**, 180402(R) (2001).

[40] M. Altarelli, M. D. Núnez-Regueiro, and M. Papoular, Phys. Rev. Lett. **74**, 3840 (1995).

[41] D. Mukamel and S. Krinsky, Phys. Rev. B **13**, 5065 (1976).

[42] D. Mukamel and S. Krinsky, Phys. Rev. B **13**, 5078 (1976).

[43] E. Brézin, J. C. Le Guillou, and J. Zinn-Justin, Phys. Rev. B **10**, 892 (1974).

[44] P. Bak, S. Krinsky, and D. Mukamel, Phys. Rev. Lett. **36**, 52 (1976).

[45] M. Bouvier, P. Lethuillier, and D. Schmitt, Phys. Rev. B **43**, 13137 (1991).

[46] A. Malachias, E. Granado, R. Lora-Serrano, and P. G. Pagliuso (unpublished).

[47] A. Aharony, Phys. Rev. B **8**, 3349 (1973).

[48] S. Henneberger, E. Frey, P. G. Maier, F. Schwabl, and G. M. Kalvius, Phys. Rev. B **60**, 9630 (1999).

[49] S. Srinath and S. N. Kaul, Phys. Rev. B **60**, 12166 (1999).

[50] J. A. Blanco, D. Gignoux, and D. Schmitt, Phys. Rev. B **43**, 13145 (1991).

[51] M. Rotter, M. Loewenhaupt, M. Doerr, A. Lindbaum, and H. Michor, Phys. Rev. B **64**, 014402 (2001).

[52] A. Aharony, Phys. Rev. B **12**, 1038 (1975).

[53] A. Weinrib and B. I. Halperin, Phys. Rev. B **27**, 413 (1983).

[54] B. Uchoa and H. Westfahl (unpublished).